Research on Engineering Structures & Materials
www.jresm.org
Research Group

Research Article

Probabilistic investigation of the pounding effect in steel moment resisting frames with equal and unequal heights

Abbasali Sadeghi[*1,a], Hamid Kazemi[2,b], Mohammad Hossein Razmkhah[3,c], Amirreza Sadeghi[4,d]

[1]*Department of Civil Engineering, Birjand Branch, Islamic Azad University, Birjand, Iran*
[2]*Department of Civil Engineering, Mashhad Branch, Islamic Azad University, Mashhad, Iran*
[3]*Department of Civil Engineering, Semnan University, Semnan, Iran*
[4]*Department of Civil Engineering, University of Birjand, Birjand, Iran*

Article Info

Article history:

Received 12 Oct 2023
Accepted 23 Mar 2024

Keywords:

Steel moment resisting frame (SMRF);
Pounding;
Gap;
Incremental dynamic analysis (IDA);
Fragility curve;
Kriging meta-model

Abstract

In this research, the influence of the pounding phenomenon of two adjacent steel moment resisting frames (SMRFs) with 2 and 5-story with an intermediate ductility is investigated by considering equal and unequal heights under seismic excitations. In this way, two scenarios are applied. The first and second scenarios are related to the pounding of two SMRFs with an equal height (both frames with 2-story) and an unequal height (2-story and 5-story frames), respectively. In the following, at first, sensitivity analysis is conducted by the Monte Carlo simulation (MCS) method. Then, the collapse performance of the studied SMRFs is evaluated by incremental dynamic analysis (IDA), and fragility curves under 14 far-fault records and also, the failure probability is predicted by the Kriging meta-model. The results of sensitivity analysis indicate that the yield strength of cross-sections and dead load were the greatest effect on failure probability computation. Also, in the statistical level of 50%, the collapse probability of SMRFs with an equal height is 17% compared to the SMRFs with an unequal height. Also, the results of the Kriging meta-model show that the failure probability is increased by 65% in an unequal height versus an equal height.

1. Introduction

Today, in cities with high population density, the minimum gap among adjacent structures is an important issue due to the fluctuation of buildings during seismic excitations, and various codes in this field have specified the minimum distance to prevent buildings from colliding [1, 2]. The conducted studies in the field of structural damage in past earthquakes show that adjacent buildings with partial discontinuity or with a common wall between two structures may suffer serious damage during an earthquake and even go to the point of collapse [3, 4]. Kamal and Inel showed that pounding phenomenon may alter the dynamic features of two adjacent buildings significantly [5]. The pounding problem was first numerically modeled for single-degree-of-freedom (SDOF) structures [6-8], and then for multi-degree-of-freedom (MDOF) structures, these analyses were performed numerically with concentrated mass [9, 10], and then for three adjacent buildings, numerical analyses related to pounding were also performed [11, 12]. Past earthquakes have shown that the pounding issue is a serious topic for tall buildings in the vicinity whose floors are not on the same level [13-17]. Another important reason for the pounding issue

*Corresponding author: abbasali.sadeghi@mshdiau.ac.ir
[a] orcid.org/0000-0002-3016-9080; [b] orcid.org/0000-0003-2590-1051; [c] orcid.org/0000-0001-5463-308X; [d] orcid.org/0009-0007-0468-7718
DOI: http://dx.doi.org/10.17515/resm2024.07ma1012rs

is that different natural frequencies of adjacent buildings may vibrate out of phase [5]. Eftychia et al. [19] evaluated the influence of base isolation on the impact of two buildings and Forcellini [20] studied the effect of the interaction of soil and structure on the pounding phenomenon. The results of this research showed that the deformation of the soil during an earthquake causes the pounding phenomenon is intensified. Also, past studies about steel moment resisting frames (SMRFs) are presented in the following. The fragility behavior of SMRFs is evaluated subjected to vehicle impact by Sadeghi et al. [21] and in another research by Sadeghi et al. [22], the weight of SMRFs is optimized under vehicle collision by using optimization algorithms. Saberi et al. [23] assessed the effect of fire on SMRFs. The results of this paper showed that by varying each of the factors, the damage modes are changed considering to the thickness of connections under fire loadings.

2. Research Significance

By reviewing past technical studies, it is revealed that the debated topic is novel and new. Therefore, in this paper, as a research significance and contribution part, the effect of pounding phenomenon between two adjacent SMRFs with equal and unequal heights has been investigated by presenting the probabilistic framework. In this way, two scenarios are utilized. The first and second scenarios are related to the pounding of two SMRFs with an equal height (both frames with 2-story) and an unequal height (2-story and 5-story frames), respectively.

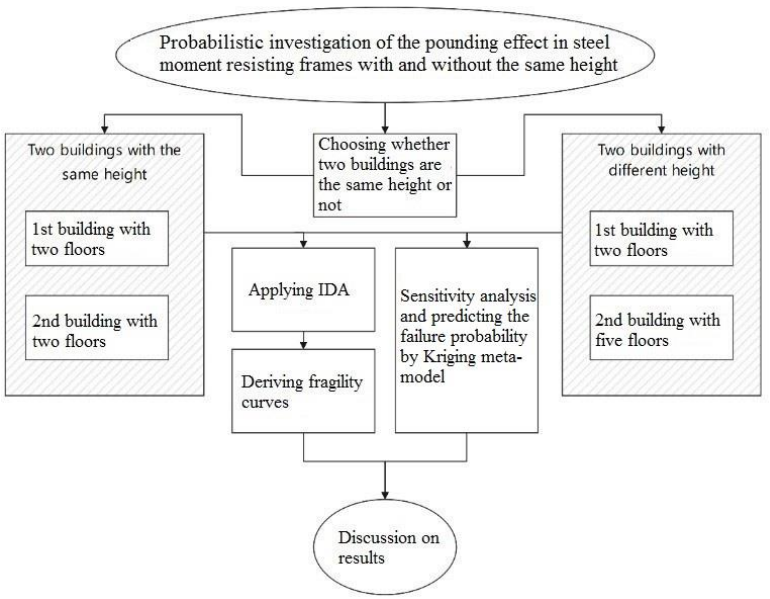

Fig. 1. The flowchart of the current research

In the following, the sensitivity analysis of random variables of SMRFs is performed under the influence of pounding phenomenon and the effective random variables are specified by using the Monte Carlo simulation (MCS) method, then, incremental dynamic analysis (IDA) has been performed in OpenSees software [24] under 14 far-fault records to evaluate this issue probabilistically, and the amount of damage has been assessed by using the fragility curves. In the following, for the first time, the Kriging meta-model is used to

predict the failure probability for studied SMRFs. It is noted that the probabilistic framework for SMRFs with and without an equal height under the effect of pounding has not been investigated from this point of view. Fig. 1 indicates the flowchart of this research.

3. Theoretical Fundamentals

In this part, the technical concepts related to present a probabilistic framework of SMRFs with equal and unequal heights under the effect of pounding phenomenon are introduced. In this route, the technical fundamentals such as IDA, fragility curves, MCS method, sensitivity analysis, and Kriging meta-model are elaborated point by point.

3.1 IDA and Fragility Curves

IDA is a probabilistic numerical method for assessing the performance of structures against seismic records. The volume of produced data is huge in this method and presents the probabilistic framework for indicating the seismic behavior of structures. In this method, the intensity of earthquake records is amplified incrementally until the structural responses of structures achieve the intended performance levels. In The following, the fragility curve expresses the probability of failure corresponding to a certain damage mode in several levels of seismic excitations. In fact, the fragility curve describes the ratio between the intensity of the earthquake and the level of possible seismic damage. To accurately determine such a ratio, it is important to choose the correct intensity of the earthquake in the location of the structure [25, 26]. In this paper, for IDA, damage measure and intensity measure are assumed to be the maximum drift ratio of the SMRFs and 5% damped first mode spectral acceleration, $S_a(T_1, 5\%)$, respectively, and fragility curves are depicted just for the collapse performance (CP) level. As a result, the collapse capacity of SMRFs with equal and unequal heights are computed under the occurrence of the pounding phenomenon. In the present research, fragility curves are depicted by assessing the results of IDAs curves, the statistical approaches are conducted in EasyFit software to extract fragility curves based on collapse limit state. For the above circumstances, fragility curves are achieved according to Eq (1) [25]:

$$Fragility\ (x) = P[S_a \geq S_{a,c} / S_a = x] = P[S_{a,c} \leq x] \quad (1)$$

In Eq (1), the function Fragility (x) is the value of the collapse limit state achieved by fragility curve for spectral acceleration (x) and showing collapse capacity of the *SMRFs*. The parameters S_a and $S_{a,c}$ are spectral acceleration and collapse capacity of *SMRFs*, respectively.

3.2 MCS Method

MCS is a probabilistic method to compute the failure probability of structures. This method is widely used in reliability engineering. According to fundamentals of this method, MCS solves structural problems by statistical sampling of random parameters in mathematical way. In this way, Eq (2) shows the failure probability (P_f) of structural problems by using MCS method. Parameters x and g (x) are named as the uncertain quantities and the performance function of the structural systems, respectively [27].

$$P_f = \int_{g(x)\leq 0}^{\blacksquare} f_x(x)dx = \int_{\mathbb{X}}^{\blacksquare} \mathbb{I}_{g(x)\leq 0}(x)\ f_x(x)\ dx = \mathbb{E}_f\ (\mathbb{I}_{g(x)\leq 0}\ (x)) \quad (2)$$

Based on Eq (2), the parameters of $\mathbb{E}_f$ *and* f_x are defined as the expectation operator and the probability density function of uncertainties x and the functions $g(x) \leq 0$ *and* $\mathbb{I}_{g(x)\leq 0}$ *are* indicated as the failure set and an index.

3.3 Sensitivity Analysis

In simulation methods, sensitivity analysis is often evaluated by computing the rate of change of failure probability to the statistical characteristics of each variable $\partial P_f / \partial P$ (P can be the mean or standard deviation of each variable) [27, 28]. The easiest way to estimate the results of sensitivity analysis by considering the simulation method is to use the MCS method based on Eq (3). By using the MCS, the rate of the above changes can be calculated with a single simulation (which estimates the failure probability) as follows:

$$\frac{\partial P_f}{\partial p} = \frac{\partial}{\partial p} \int I[g\,(x) < 0]\, f_{x(p)}(x) dx \tag{3}$$

In Eq (3), (f_x) is the probability density function of parameters and (I) is the counter vector. The need to derive the probability density function is one of the disadvantages of estimating sensitivity results by using Eq (3).

3.4 Kriging Meta-Model

The status of structural systems such as SMRF is evaluated in terms of reliability analysis by computing the failure probability mathematically. These failure probabilities are usually determined by structural damage levels. Therefore, the Kriging meta-model is an interpolation method to predict the response of specific data. Kriging meta-model approximates a function using a combination of basis functions. For interested readers, the surplus explanations about this method are presented in reference [27].

4. Modeling Verification

In this research, to verify the modeling procedure of the pounding phenomenon, the extracted results of OpenSees software are compared with the experimental results of Takabatake et al. (2014) [29]. In this regard, the investigated models are two three-dimensional 4-story samples with one span named F-A and F-B, 4. The global dimensions of these frames are 0.20 m, 0.15 m, and 0.60 m for width, depth and height, respectively. For more information about the features of experimental models, interested readers can refer to the research of Takabatake et al. (2014) [29]. The schematic view of the adjacent frames is presented in Fig. 2. The experimental and numerical models are indicated in Fig. 2 (a) and (b), respectively. In this research, for structural members, fiber cross-section has been used as an extended plasticity model. In these members, instead of the plasticization of the materials in certain points of the structure (such as points in the beam, which is near the column), the plasticization of the materials is considered distributed throughout the length of the member. In current paper, non-linear force beam-column members have been used to model the beam and column members. In the following, the number of threaded sections is 200 and the number of integration points along the length of the beam-column members is assumed to be 5. In the following, nonlinear dynamic time history analysis is conducted under the El-Centro earthquake record (1940). This record is scaled based on the maximum acceleration of 0.5 m/sec^2. Also, the number of time steps is equal to 6000 with a step of one to ten thousand. The considered damping for the models is as described in Reference [29]. In this regard, a model ELCN 2-0-0 in which only impact effects between two structures were included was selected to verify the results of analytical modeling. In addition, the GAP element has been used between two structures instead of the aluminum element. The comparison of the numerical modeling results of this paper and the reference model [29] is presented in Tables 1 and 2. In Table 1, the percentage of conformity of the period results of the reference model and the constructed model in OpenSees software is presented and in Table 2, the percentage of conformity of the maximum impact force of the two experimental and numerical models are compared with each other. The error rate of numerical modeling process versus Experimental setup in period and maximum impact

force is 3.48% and 3.19%, respectively. As a result, the outputs of the numerical modeling are in good agreement with the experimental results.

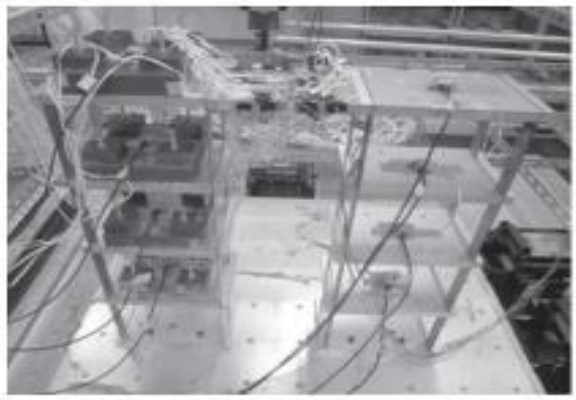

(a)

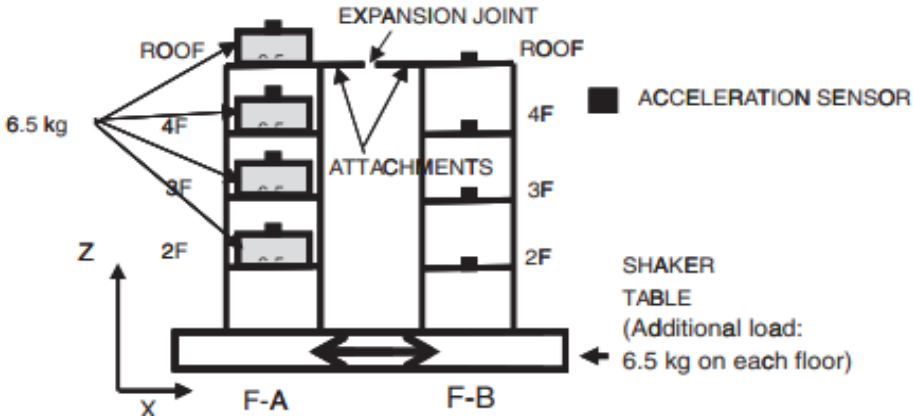

(b)

Fig. 2. The process of experiment [29] (a) The global view of experimental setup, (b) The schematic view of pounding phenomenon

Table 1. The comparison of period values of numerical and reference model [29]

Sample	F-A	F-B
Reference paper [29]	0.287 sec	0.135 sec
Present paper	0.277 sec	0.124 sec
Error rate (%)	3.48	8.14

Table 2. The comparison of maximum impact force values of numerical and reference model

Outputs	Maximum impact force
Reference paper [29]	61.48 kN
Present paper	63.51 kN

Error rate (%)	3.19

5. Modeling Procedure

In this study, 2 and 5-story SMRFs with intermediate ductility are designed based on ASCE07 [30] and AISC-360 [31]. Soil type D is considered for the designing procedure. The seismicity of the model was very high with high importance. The values of 1500 and 600 kg/m^2 are assumed for dead and live loads, respectively. The used steel in the structural components was ST37 with values of 200 GPa, 240 MPa, and 370 MPa for elasticity modulus, yield stress, and ultimate stress, respectively. For structural modeling, the Steel01 model is considered with a post-yielding stiffness of 3% [32]. Fig. 3 shows the building plan and determination of the exterior frame enclosed in the red rectangle. Fig. 4 (a) and (b) indicates the two-dimensional elevation of SMRFs with 2 and 5-story, respectively. Also, the designed cross-sections of structural components are introduced in Table 3.

In this research, to evaluate the performance of adjacent SMRFs under the effect of pounding caused by an earthquake, as equal height samples, two adjacent 2-story SMRFs and as unequal height samples, two adjacent 2 and 5-story SMRFs are considered. In modeling the impact of two frames on each other, the gap between the two frames is used according to the relations provided in ASCE07 [30].

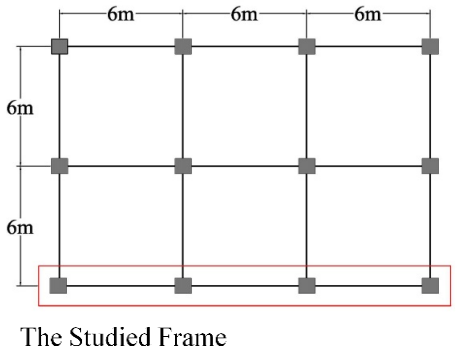

Fig. 3. Building plan view and location of the studied frame

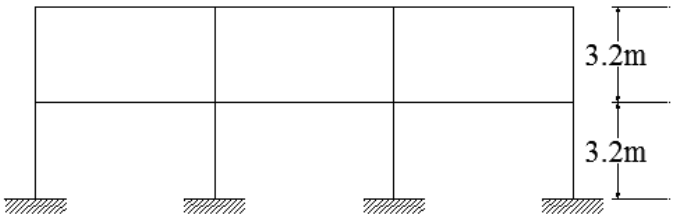

(a)

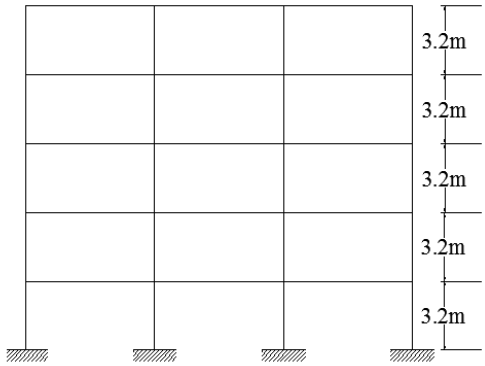

(b)

Fig. 4. The two-dimensional elevation of the studied models (a) 2-story SMRF, (b) 5-story SMRF

For simulating the gap in this research, the nonlinear viscoelastic model is used [33, 34]. The Hertz contact model is utilized to consider the energy loss during impact. According to Fig. 5, a non-linear damper is built in parallel with the non-linear spring in this model and damping is omitted during the return phase. Therefore, energy loss in the return phase is not considered. ZeroLength element is used for impact modeling.

Table 3. The designed cross sections of structural components of the studied SMRFs

SMRF	Story	Beam		Column	
		Side span	Middle span	Side span	Middle span
2-story	1st story	IPE200	IPE220	BOX200*20	BOX200*20
	2nd story	IPE180	IPE200	BOX200*18	BOX200*18
5-story	1st story	IPE260	IPE280	BOX200*22	BOX200*25
	2nd story	IPE260	IPE260	BOX200*20	BOX200*22
	3rd story	IPE240	IPE260	BOX200*18	BOX200*20
	4th and 5th stories	IPE220	IPE240	BOX200*16	BOX200*16

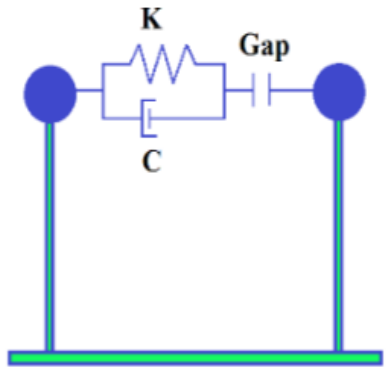

Fig. 5. The schematic of pounding model in adjacent SMRFs [33]

This element is used to connect two nodes. In this element, until the gap between the two structures is filled, no force is created and the amount of slip and damping is zero. After two structures collide with each other and by creating compression in the spring, a negative (compressive) force is created. After the separation of the two structures, the force returns to zero and no force is transferred in the tension state. For this element, elastoplastic properties are used in OpenSees software. Finally, Figs. 6 and 7 illustrate the configuration of two adjacent SMRFs with and without an equal height.

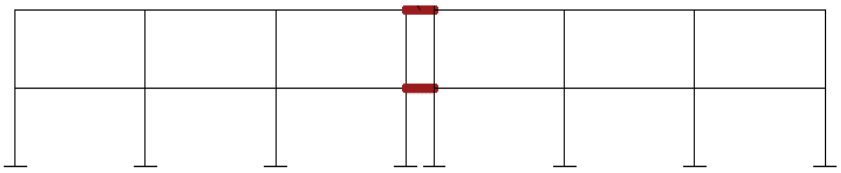

Fig. 6. The configuration of two adjacent SMRFs with an equal height

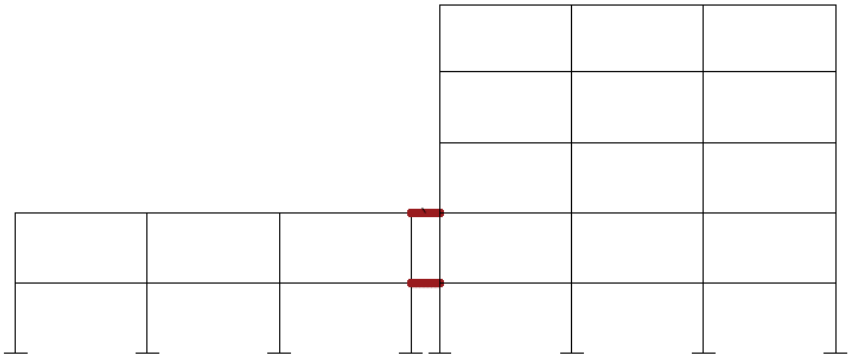

Fig. 7. The configuration of two adjacent SMRFs with an unequal height

5.1 Limit State Function

In this study, the failure probability is calculated based on the Kriging meta-model, taking into account the structural uncertainties for the pounding scenarios of adjacent SMRFs. To calculate the failure probability, since the considered structural system is non-linear, simulation methods are used to increase the accuracy. Therefore, it is necessary to determine the points in the health and failure areas first. For this purpose, the limit state function (LSF) of the reliability problem should be evaluated by structural analysis. At each time of structural analysis, random variables are defined according to Table 4 for the investigated structural models under the scenario of pounding of adjacent SMRFs based on the selected distribution. To save time, before calculating the failure probability, a sensitivity analysis is done and the random variables that have a negligible dependence on the change of the LSF are removed and other influential variables are considered definitively. The proposed LSF for the investigated models in this research is presented in the scenario of pounding of the adjacent SMRFs according to Eq (4):

$$g_1 = 0.1 - (Max(Drift)) \tag{4}$$

In Eq (4), Max (Drift) is the maximum drift of the structure at each time of analysis and the value of 0.1 is the collapse limit of the structure based on the regulations. Now, if $g_1>0$ after

the analysis, the sample is in the healthy area, and if $g_1 \leq 0$, the sample is in the failure area. According to the different seismic codes, the values of drift equivalent to different performance levels of SMRFs have been presented [35, 36]. In transient deformations, drifts of 0.7%, 2.5%, 5%, and 10% show Immediate Occupancy (IO), Life Safety (LS), Collapse Prevention (CP), and Collapse (C) performance levels, respectively.

Table 4. The statistical features of random variables in this study

Category	Symbol	Description	Unit	PDF	Mean	c. o. v or σ	Reference
Gravity Load	DL	Dead load	kg/m	N*	1500	0.1	[37, 38]
	LL	Live load	kg/m	G*	600	0.4	[37, 38]
Material	F_y	Yield strength	MPa	LN*	240	0.07	[37, 39]
	E	Elasticity modulus	MPa	LN	$2*10^5$	0.03	[40, 41]
	ξ	Damping ratio	-	LN	5%	40	[41]
	ρ	Specific weight	kg/m³	LN	7890	0.1	[39]
	ϑ	Poisson ratio	-	LN	0.3	0.1	[39]
Geometric	L	Beam length	m	N	6	0.0304	[39, 40]
	H	Column height	m	N	3.2	0.0304	[39, 40]

* N: Normal, LN: Lognormal, G: Gamma

5.2 Ground Motion Records

One of the main issues in evaluating the nonlinear dynamic analysis of structures is the selection of earthquakes and their number to obtain the results with appropriate accuracy. FEMA P 695 [42] suggests a set of near-fault and far-fault earthquake records for nonlinear dynamic analyses. This code presents the suitable earthquake records with different natures for calculating the collapse probability of structure. In this study, IDA has been performed with small and controlled steps.

Table 5. The features of the studied earthquakes

ID No.	Date	Event	Station	Magnitude (M_w)	Component	PGA[1] (g)	PGV[2] (cm/s²)
R1	1994	Northridge, CA	Beverly Hills-Mulhol	6.7	NORTH/ MUL009	0.42	59
R2					NORTH/ MUL279	0.52	63
R3	1994	Northridge, CA	Canyon Country-WLC	6.7	000	0.41	43
R4					NORTH/ LOS270	0.48	45
R5	1999	Duzce, Turkey	Bolu	7.1	DUZCE/ BOL000	0.73	56
R6					DUZCE/ BOL090	0.82	62
R7	1999	Hector Mine, CA	Hector	7.1	HECTOR/ HEC000	0.27	29
R8					HECTOR/ HEC090	0.34	42

R9	1979	Imperial Valley, CA	Delta	6.5	IMPVAL/ H-DLT262	0.24	26
R10					IMPVAL/ H-DLT352	0.35	33
R11	1979	Imperial Valley, CA	El Centro Array # 11	6.5	IMPVAL/ H-E11140	0.36	35
R12					IMPVAL/ H-E11230	0.38	42
R13	1995	Kobe, Japan	Nishi-Akashi	6.9	KOBE/ NIS000	0.50	37
R14					KOBE/ NIS090	0.51	37

[1] Peak ground acceleration
[2] Peak ground velocity

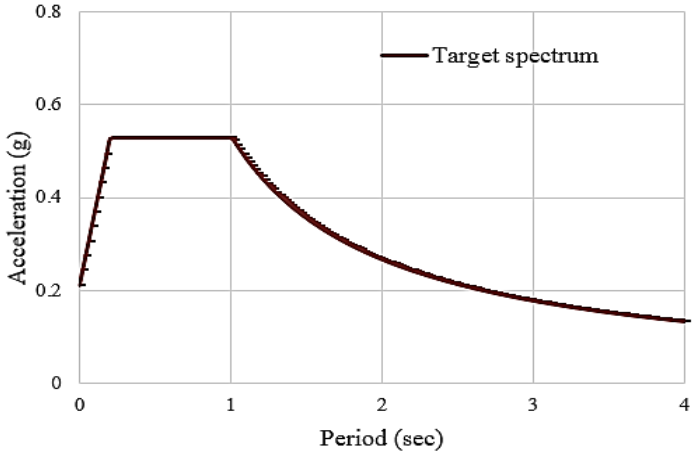

Fig. 8. Target spectrum of ASCE07 [30]

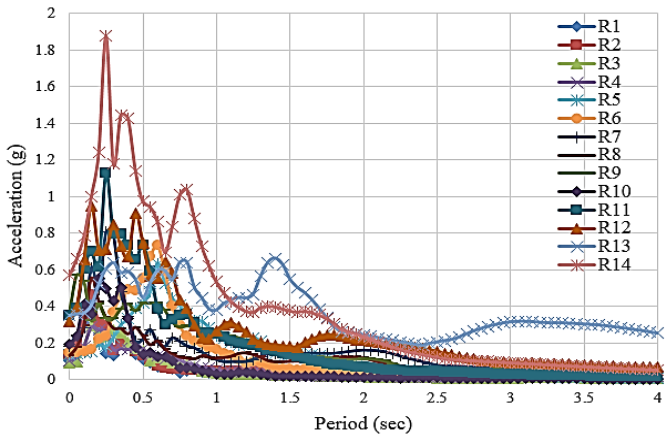

Fig. 9. Elastic acceleration spectrum for 5% damping of earthquake records used in this research

It is noted that IDA is a set of time history nonlinear dynamic analyses under different numerous records therefore selection of seismic records is an important step to assess the performance of structures probabilistically. Some researchers evaluate the influence of the

features, content and number of the seismic excitations on the analysis results [43-50]. In this paper, these records are first scaled according to the peak ground velocity (PGV). Then, the spectral acceleration of all records in the period of the first mode of the structure (S_a (T_1, 5%)) was scaled. Also, target spectrum and an elastic acceleration spectrum for 5% damping of earthquake records used in this research are depicted based on Figs. 8 and 9. In this study, IDA is performed and IDA curves are plotted. In the following, for calculating the seismic collapse capacity, the fragility curves of SMRFs adjacent to each other in two scenarios are obtained. Table 5 shows the features of the studied earthquakes.

6. Results and Discussion

6.1 Results of The Sensitivity Analysis

In this part, the sensitivity analysis of random parameters of studied SMRFs such as dead load, live load, yield strength, elasticity modulus, damping ratio, specific weight, Poisson ratio, beam length, and column height is checked by MCS method. In this way, the variation rate of failure probability to the statistical characteristics of each mentioned variable is assessed. The sensitivity analysis is performed by calling the LSF 100,000 times and by evaluating the rate of change of the failure probability compared to the changes of each random parameter, and the results of the sensitivity analysis are also presented in Table 6. It can be seen that for the desired models under the effect of pounding, the parameters with uncertainty of the yield strength of the cross-sections, and the dead load have the greatest effect and Poisson's ratio, the specific weight of the cross-sections, and the live load have the least effect on the calculation of failure probability.

Table 6. The results of the sensitivity analysis of the SMRF models under the effect of pounding

No.	Failure Probability Variation for Each Variable	
1	$(\partial Pf)/(\partial DL)$	0.0086146
2	$(\partial Pf)/(\partial LL)$	0.000064689
3	$(\partial Pf)/(\partial Fy)$	-0.032309
4	$(\partial Pf)/(\partial E)$	0.000090022
5	$(\partial Pf)/(\partial \xi)$	-0.000075751
6	$(\partial Pf)/(\partial \rho)$	-0.00006656
7	$(\partial Pf)/(\partial \vartheta)$	0.000037615
8	$(\partial Pf)/(\partial L)$	0.00021061
9	$(\partial Pf)/(\partial H)$	0.00066004

6.2 Results of IDA and Fragility Curves

According to Figs. 10 and 11, IDA curves of SMRFs with equal and unequal heights are presented under 7 pairs of far-fault earthquake records (equivalent to 14 earthquake record components) in OpenSees software. In addition, the fragility curves of the mentioned models are shown in Fig. 12.

According to Fig. 12, it can be seen that the seismic collapse capacity of SMRFs adjacent to each other with equal heights is high and they have more values of spectral acceleration versus adjacent SMRFs with unequal heights. Table 7 shows the spectral accelerations of the mentioned SMRFs for different statistical levels of 16%, 50%, and 84%.

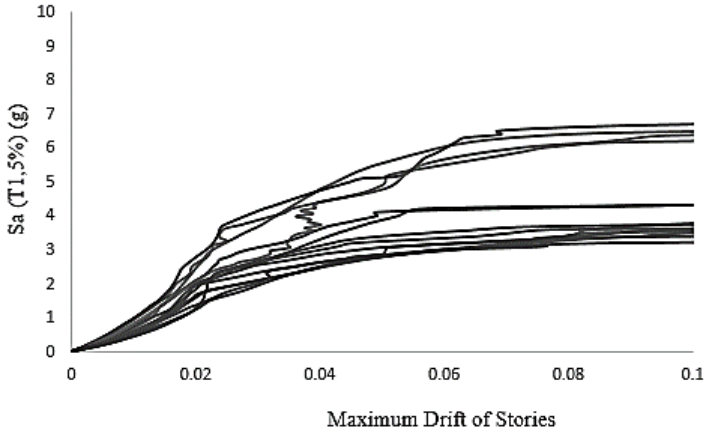

Fig. 10. IDA curves of two adjacent SMRFs with an equal height

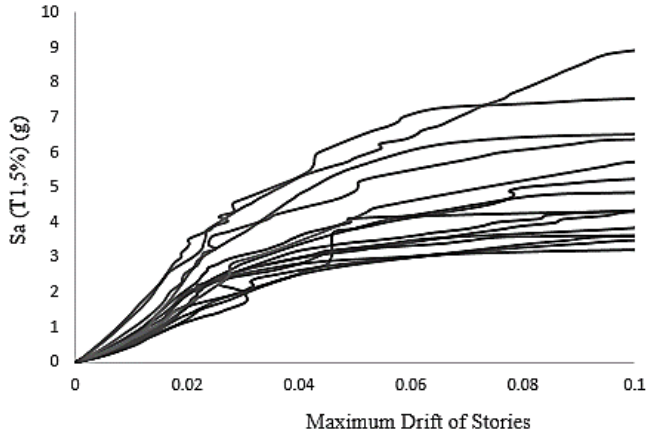

Fig. 11. IDA curves of two adjacent SMRFs with an unequal height

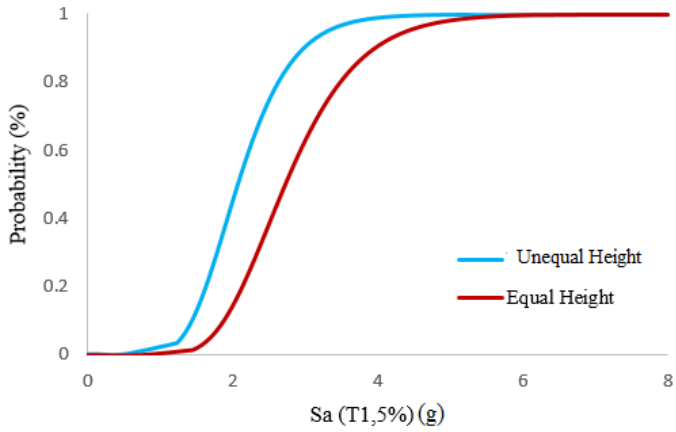

Fig. 12. Fragility curves of two adjacent SMRFs with the equal and unequal heights

Also, by conducting numerous time history nonlinear dynamic analyses, the comparison of maximum values of story displacement, story drift, story acceleration, and impact force of two adjacent SMRFs with the equal and unequal heights are reported based on Figs. 13 to 16. The extracted seismic responses of the studied models indicate that critical values of story displacement, story drift, story acceleration, and impact force are related to the two adjacent SMRFs with the unequal heights.

Table 7. The spectral acceleration of SMRFs under the effect of pounding

Statistical levels	SMRFs with equal heights (g)	SMRFs with unequal heights (g)
16%	2	1.6
50%	2.3	1.9
84%	3.9	2.4

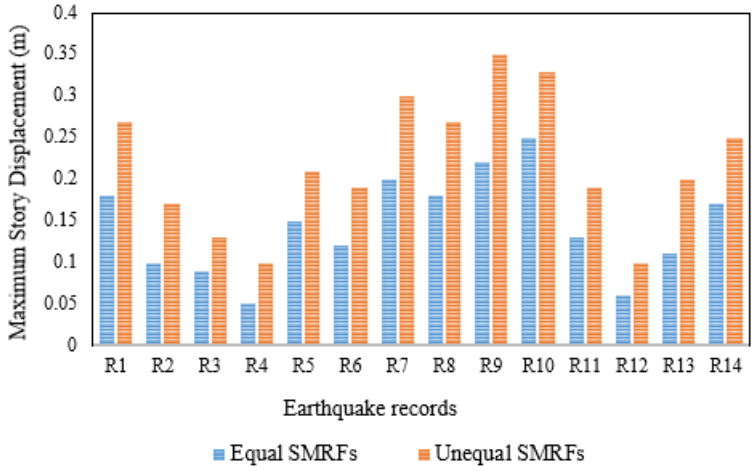

Fig. 13. Comparison of maximum story displacement of two adjacent SMRFs with the equal and unequal heights

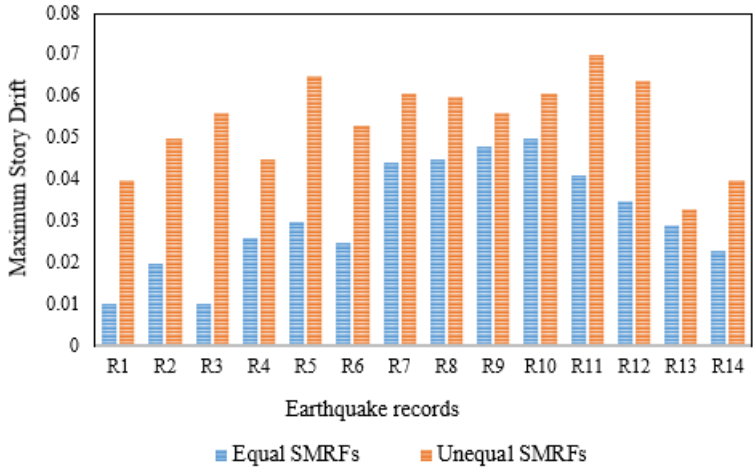

Fig. 14. Comparison of maximum story drift of two adjacent SMRFs with the equal and unequal heights

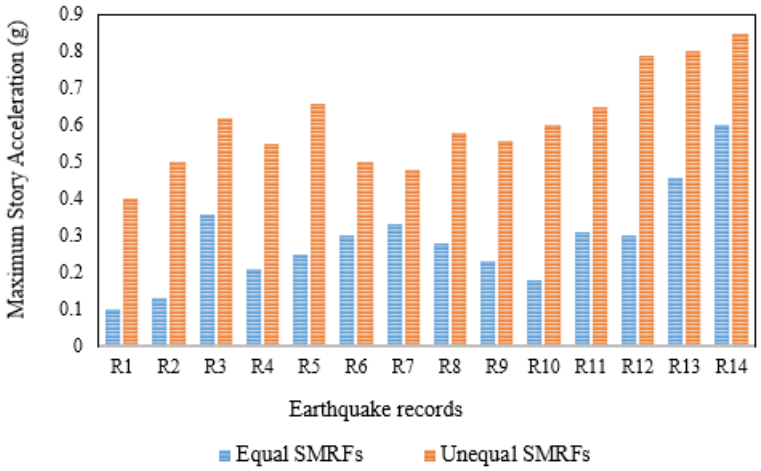

Fig. 15. Comparison of maximum story acceleration of two adjacent SMRFs with the equal and unequal heights

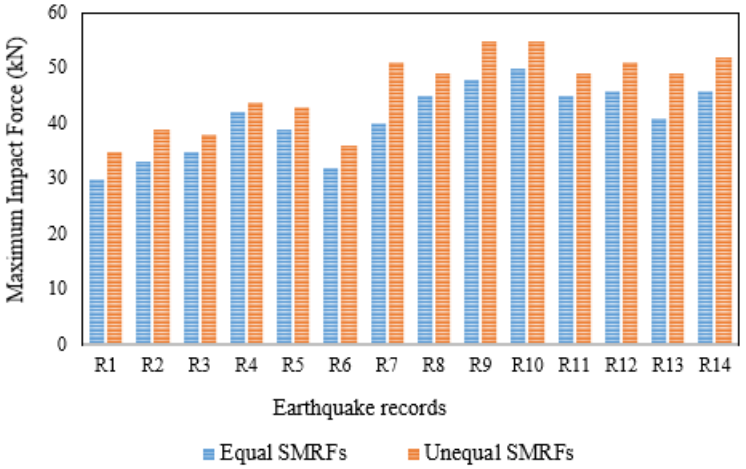

Fig. 16. Comparison of maximum impact force of two adjacent SMRFs with the equal and unequal heights

6.3 Results of Kriging Meta-Model

In this study, for preparing the meta-model, 3000 random samples are produced based on the statistical distribution of each random parameter placed in Table 4. Since the LSF of this research is based on drift. As a result, the drift of selected SMRFs is computed and in this regard, 2000 random samples and the corresponding drift of mentioned SMRFs are opted to train the Kriging meta-model. The remaining samples are utilized to test the Kriging meta-model for predicting the drift values of SMRFs based on LSF. In the following, MCS with 100,000 simulations is conducted for evaluating the reliability of the SMRFs with the equal and unequal heights. The accuracy of the findings given by the Kriging meta-model can be verified by the MCS. Table 8 indicates the results of the reliability analysis of the SMRFs with the equal and unequal heights by using MCS and Kriging meta-model. By comparing the results in Table 8, it is clear that Kriging meta-model can predict the failure probability of SMRFs with the equal and unequal heights by high validity, and accuracy versus MCS, and It can significantly decrease the computational time with far fewer the

number of samples than MCS. It is also found that the results of SMRFs with equal heights have a higher reliability index than the SMRFs with unequal heights. Also, It is noted that the parameters such as (β), (P_f), and (#g call) are the reliability index, failure probability, and the number of calling LSF, respectively.

Table 8. Reliability analysis results of the studied SMRFs using the MCS and Kriging meta-model

	SMRFs with equal heights		SMRFs with unequal heights	
Simulation Method	MCS	Kriging	MCS	Kriging
β	2.80	2.79	2.64	2.63
P_f	2.5×10^{-3}	2.6×10^{-3}	4.2×10^{-3}	4.3×10^{-3}
#g call	10^5	2000	10^5	2000

It is noted that the reliability analysis using the MCS method with 100,000 simulations is really time consuming therefore the Kriging meta-model can decrease the computational time significantly in comparison with MCS. In the following, by using Kriging meta-model, taking into account the uncertainties based on Table 4, the failure probability values of SMRFs with equal and unequal heights are extracted due to 14 far-fault earthquake records. These values are specified in Table 9. The total results of Table 9 indicate that the failure probability of SMRFs with an unequal height is high in comparison of SMRFs with an equal height.

Table 9. The failure probabilities of SMRFs under the effect of pounding by using Kriging meta-model

No.	SMRFs with an equal height	SMRFs with an unequal height
1	0.0026	0.0043
2	0.0021	0.0035
3	0.0024	0.0040
4	0.0022	0.0042
5	0.0022	0.0041
6	0.0018	0.0033
7	0.0017	0.0035
8	0.0021	0.0032
9	0.0015	0.0036
10	0.0022	0.0040
11	0.0024	0.0039
12	0.0018	0.0036
13	0.0024	0.0035
14	0.0021	0.0029

7. Conclusions

Pounding is one of the most common phenomenon during an earthquake that causes significant damage to adjacent SMRFs. In this research, SMRFs with the equal and unequal heights are placed adjacent to each other, taking into account the gap, and their failure probability is calculated by using nonlinear dynamic analyses and Kriging meta-model. Sensitivity analysis is done to specify the important variables in failure probability

computation. Also, by using IDA and fragility curves, the collapse capacity is determined at different statistical levels. The key findings of this paper are presented in the following:

- The sensitivity analysis indicates that the variables with uncertainty of the yield strength of the cross-sections and the dead load have the greatest effect and Poisson's ratio, the specific weight of the cross-sections, and the live load have the least effect on the calculation of failure probability.
- The collapse capacity of the adjacent SMRFs with the equal heights has increased at the statistical levels of 16%, 50%, and 84% compared to the adjacent SMRFs with the unequal heights by 20%, 17%, and 90%, respectively.
- For different spectral accelerations, the collapse probability of the adjacent SMRFs with the unequal height is higher than that of equal height.
- The results of Kriging meta-model indicate that the failure probability is increased by 65% in SMRFs with an unequal height versus an equal height.
- The results of reliability analysis and fragility curves reveal that the collapse capacity of the adjacent SMRFs with the equal height is higher than that of unequal height.
- The application of Kriging meta-model is confirmed with MCS. This meta-model can decrease the computational time significantly in comparison with MCS. Hence, Kriging is an exact probabilistic way for reliability assessment of pounding issues in adjacent SMRFs.
- As recommendations for future works, the authors propose to assess the seismic performance of the adjacent SMRFs with the equal and unequal heights (various stories) under the influence of pounding by considering soil-structure-interaction (SSI) by using reliability and fragility analyses.

References

[1] Favvata MJ. Minimum required separation gap for adjacent RC frames with potential inter-story seismic pounding**.** Engineering Structures, 2017; 152: 643-659**.** https://doi.org/10.1016/j.engstruct.2017.09.025

[2] Lin JH. Separation distance to avoid seismic pounding of adjacent buildings. Earthquake engineering & structural dynamics, 1997; 26(3): 395-403. https://doi.org/10.1002/(SICI)1096-9845(199703)26:3%3C395::AID-EQE655%3E3.0.CO;2-F

[3] Kasai K, Maison BF. Building pounding damage during the 1989 Loma Prieta earthquake. Engineering structures, 1997; 19(3): 195-207**.** https://doi.org/10.1016/S0141-0296(96)00082-X

[4] Sorrentino L, Cattari S, Da Porto F, Magenes G, Penna A. Seismic behaviour of ordinary masonry buildings during the 2016 central Italy earthquakes. Bulletin of Earthquake Engineering, 2019; 17(10): 5583-5607**.** https://doi.org/10.1007/s10518-018-0370-4

[5] Kamal M, Inel M. Simplified approaches for estimation of required seismic separation distance between adjacent reinforced concrete buildings. Engineering Structures, 2022; 252: 113610**.** https://doi.org/10.1016/j.engstruct.2021.113610

[6] Naderpour H, Barros R, Khatami S, Jankowski R. Numerical study on pounding between two adjacent buildings under earthquake excitation. Shock and vibration, 2016. https://doi.org/10.1155/2016/1504783

[7] Anagnostopoulos SA. Pounding of buildings in series during earthquakes. Earthquake engineering & structural dynamics, 1988; 16(3): 443-456**.** https://doi.org/10.1002/eqe.4290160311

[8] Jankowski R. Impact force spectrum for damage assessment of earthquake-induced structural pounding. Key Engineering Materials, 2005; 293: 711-718**.** https://doi.org/10.4028/www.scientific.net/KEM.293-294.711

[9] Anagnostopoulos SA, Spiliopoulos KV. An investigation of earthquake induced pounding between adjacent buildings. Earthquake engineering & structural dynamics, 1992; 21(4): 289-302. https://doi.org/10.1002/eqe.4290210402
[10] Maison BF, Kasai K. Dynamics of pounding when two buildings collide. Earthquake engineering & structural dynamics, 1992; 21(9): 771-786. https://doi.org/10.1002/eqe.4290210903
[11] El-Khoriby S, Seleemah A, Elwardany H, Jankowski R. Experimental and numerical study on pounding of structures in series. Advances in Structural Engineering: Dynamics, 2015: 1073-1089. https://doi.org/10.1007/978-81-322-2193-7_84
[12] Jankowski R, Seleemah A, El-Khoriby S, Elwardany H. Experimental study on pounding between structures during damaging earthquakes. Key Engineering Materials, 2015; 627: 249-252. https://doi.org/10.4028/www.scientific.net/KEM.627.249
[13] Stone WC, Yoke FY, Celebi M, Hanks T, Leyendecker EV. Engineering Aspects of the September 19, 1985 Mexico Earthquake (NBS BSS 165), 1987.
[14]Kasai K, Jeng V, Patel P, Munshi J, Maison B. Seismic pounding effects-survey and analysis. Earthquake Engineering, 1992.
[15] Cole G, Dhakal R, Carr A, Bull D. Interbuilding pounding damage observed in the 2010 Darfield earthquake. Bulletin of the New Zealand Society for Earthquake Engineering, 2010; 43(4): 382-386. https://doi.org/10.5459/bnzsee.43.4.382-386
[16] Cole G, Dhakal R, Chouw N. Building Pounding Damage Observed in the 2011 Christchurch earthquake Christchurch Earthquake. Earthquake Engng Struct Dy, 2012; 41(5): 893-913. https://doi.org/10.1002/eqe.1164
[17] Dizhur D, et al., Performance of masonry buildings and churches in the 22 February 2011 Christchurch earthquake. Bulletin of the New Zealand Society for Earthquake Engineering, 2011; 44(4): 279-296. https://doi.org/10.5459/bnzsee.44.4.279-296
[18] Maniatakis CA, Spyrakos CC, Kiriakopoulos PD, Tsellos KP. Seismic response of a historic church considering pounding phenomena. Bulletin of Earthquake Engineering, 2018; 16: 2913-2941. https://doi.org/10.1007/s10518-017-0293-5
[19] Mavronicola EA, Polycarpou PC, Komodromos P. Effect of ground motion directionality on the seismic response of base isolated buildings pounding against adjacent structures. Engineering Structures, 2020; 207: 110202. https://doi.org/10.1016/j.engstruct.2020.110202
[20] Forcellini D. The role of Soil Structure Interaction (SSI) on the risk of pounding between low-rise buildings. Structures, 2023; 56: 105014. https://doi.org/10.1016/j.istruc.2023.105014
[21] Sadeghi A, Kazemi H, Mehdizadeh K, Jadali F. Fragility analysis of steel moment-resisting frames subjected to impact actions. Journal of Building Pathology and Rehabilitation, 2022; 7(26). https://doi.org/10.1007/s41024-022-00165-2
[22] Sadeghi A, Kazemi H, Samadi M. Single and multi-objective optimization of steel moment-resisting frame buildings under vehicle impact using evolutionary algorithms. Journal of Building Pathology and Rehabilitation, 2021; 6(21). https://doi.org/10.1007/s41024-021-00117-2
[23] Saberi H, Saberi V, Khodamoradi N, Pouraminian M, Sadeghi A. Effect of detailing on performance of steel T-connection under fire loading. Journal of Building Pathology and Rehabilitation, 2022; 7(7). https://doi.org/10.1007/s41024-021-00147-w
[24] OpenSees, Open System for Earthquake Engineering Simulation Manual, Pacific Earthquake Engineering Research Center, University of California, Berkeley, CA, 2007. http://opensees.berkeley.edu
[25] Mehdizadeh K, Karamodin A, Sadeghi A. Progressive sidesway collapse analysis of steel moment-resisting frames under earthquake excitations. Iranian Journal of Science and Technology, Transactions of Civil Engineering, 2020; 44: 1209-1221. https://doi.org/10.1007/s40996-020-00374-0

[26] Yancheshmeh BS, Adeli MM. A probabilistic approach for seismic demand estimation of steel moment frames considering capacity uncertainty. Asian J Civ Eng, 2023; 24: 2669–2691. https://doi.org/10.1007/s42107-023-00623-3
[27] Sadeghi A, Kazemi H, Samadi M. Reliability and Reliability-based Sensitivity Analyses of Steel Moment-Resisting Frame Structure subjected to Extreme Actions. Frattura ed Integrità Strutturale, 2020; 15(57): 138–159. https://doi.org/10.3221/IGF-ESIS.57.12
[28] Naji A. Sensitivity and fragility analysis of steel moment frames subjected to progressive collapse. Asian J Civ Eng, 2018; 19: 595–606. https://doi.org/10.1007/s42107-018-0045-0
[29]Takabatake H, Yasui M, Nakagawa Y, Kishida A. Relaxation method for pounding action between adjacent buildings at expansion joint. Earthq Eng Struct Dyn, 2014; 43(9): 1381–1400. https://doi.org/10.1002/eqe.2402
[30] ASCE07, Minimum design loads for buildings and other structures, New York: American Society of Civil Engineers, 2016.
[31] AISC 360, Specifications for structural steel buildings, Chicago: American Institute of Steel Construction, 2016.
[32] Kim J, Park J, Lee T. Sensitivity analysis of steel buildings subjected to column loss. Engineering Structures, 2011; 33(2): 421–432. https://doi.org/10.1016/j.engstruct.2010.10.025
[33] Madani B, Behnamfar F, TajmirRiahi H. Dynamic response of structures subjected to pounding and structure–soil–structure interaction. Soil Dynamics and Earthquake Engineering, 2015; 78: 46–60. https://doi.org/10.1016/j.soildyn.2015.07.002
[34] Jankowski R. Non-linear viscoelastic modelling of earthquake-induced structural pounding. Earthquake Eng Struct Dynam, 2005; 34(6): 595–611. https://doi.org/10.1002/eqe.434
[35] FEMA 356, Pre-Standard and Commentary for the seismic Rehabilitation of Buildings, Washington D.C. Federal Emergency Management Agency, USA, 2000.
[36] FEMA 273, NEHRP Guidelines for Seismic Rehabilitation of Buildings, Washington, D.C. Federal Emergency Management Agency, USA, 1997.
[37]Javidan MM, Kang H, Isobe D, Kim J. Computationally efficient framework for probabilistic collapse analysis of structures under extreme actions. Engineering Structures, 2018; 172, 440–452. https://doi.org/10.1016/j.engstruct.2018.06.022
[38] Ellingwood B, Galambos TV, MacGregor JG, Cornell CA. Development of a probability based load criterion for American National Standard A58 – building code requirement for minimum design loads in buildings and other structures. Washington, DC: National Bureau of Standards, Dept. of Commerce, 1980.
[39] JCSS, Joint Committee on Structural Safety, Probabilistic model code, 2001.
[40] CEN, European Committee for Standardization, EN 10034:1993.
[41] Zhang X, Liu J, Yan Y, Pandey M. An Effective Approach for Reliability-Based Sensitivity Analysis with the Principle of Maximum Entropy and Fractional Moments. Entropy, 2019; 21(7): 649. https://doi.org/10.3390/e21070649
[42]FEMA P695. Quantification of building seismic performance factors, Federal Emergency Management Agency, Washington, DC, USA, 2009.
[43] Iervolino I, Maddaloni G, Cosenza E. Eurocode-8 compliant real record sets for seismic analysis of structures. J Earthq Eng, 2008; 12:54–90. https://doi.org/10.1080/13632460701457173
[44] Kayhan AH, Demir A, Palanci M. Multi-functional solution model for spectrum compatible ground motion record selection using stochastic harmony search algorithm. Bull Earthquake Eng, 2022; 20: 6407–6440. https://doi.org/10.1007/s10518-022-01450-8

[45] Iervolino I, Maddaloni G, Cosenza E. A note on selection of time-histories for seismic analysis of bridges in Eurocode 8. J Earthq Eng, 2009; 13(8):1125–1152. https://doi.org/10.1080/13632460902792428
[46] Kayhan AH, Demir A, Palanci M. Statistical evaluation of maximum displacement demands of SDOF systems by code-compatible nonlinear time history analysis. Soil Dyn Earthq Eng, 2018;115:513–30. https://doi.org/10.1016/j.soildyn.2018.09.008
[47] Reyes JC, Kalkan E. How many records should be used in an ASCE/SEI-7 ground motion scaling procedure? Earthq Spectra, 2012; 28(3):1223–42. https://doi.org/10.1193/1.4000066
[48] Demir A. Investigation of the effect of real ground motion record number on seismic response of regular and vertically irregular RC frames. Structures, 2022; 39: 1074–91. https://doi.org/10.1016/j.istruc.2022.03.091
[49] Demir A, Palanci M, Kayhan AH. Evaluation of Supplementary Constraints on Dispersion of EDPs Using Real Ground Motion Record Sets. Arab J Sci Eng, 2020; 45: 8379–8401. https://doi.org/10.1007/s13369-020-04719-9
[50] Demir A, Kayhan AH, Palanci M. Response- and probability-based evaluation of spectrally matched ground motion selection strategies for bi-directional dynamic analysis of low- to mid-rise RC buildings. Structures, 2023; 58. https://doi.org/10.1016/j.istruc.2023.105533